10096 *Macromolecules* **2010**, *43*, 10096–10106
DOI: 10.1021/ma101805d

Macromolecules
ARTICLE

Theory of Side-Chain Liquid Crystal Polymers: Bulk Behavior and Chain Conformation

Rui Wang and Zhen-Gang Wang*

Division of Chemistry and Chemical Engineering, California Institute of Technology, Pasadena, California 91106, United States

Received August 8, 2010; Revised Manuscript Received October 19, 2010

ABSTRACT: We study the thermodynamics and chain conformation of side-chain liquid crystal polymers (SCLCPs) in the bulk using the self-consistent-field approach and a new model to account for the coupling between the orientation of the side-chain liquid-crystal (LC) groups and that of the backbone segments. The new model accounts for both a global coupling between the polymer backbone and the nematic field and a local coupling between the polymer backbone and its attached LC group. Here, the terms global and local refer to the chemical (backbone) distance between the groups. A phenomenological parameter is introduced to represent the coupling strength and nature of the attachment, i.e., end-on vs side-on. The nematic field is shown to control the chain conformation through both the global and the local coupling effects. For the side-on SCLCPs, these two coupling effects act cooperatively so that the chain conformation is always prolate. For the end-on SCLCPs, these two effects act competitively. The chain conformation can be either oblate or prolate in this case, and depends on the relative strengths of these two couplings. On the other hand, the chain conformation also affects the nematic field, primarily through the global coupling. The prolate conformation enhances the nematic field and increases the phase transition temperature, whereas the oblate conformation frustrates the nematic field and decreases the transition temperature. The nematic order parameter is found to be determined mainly by the reduced temperature, and is not sensitive to the coupling effects. Furthermore, we show that the grafting density of the LC side groups has a significant effect on the chain conformation due to the orientational competition between the LC attached and unattached segments. For the end-on SCLCPs with lower graft density, the conformation of the chain backbone can be oblate at higher temperatures and prolate at lower temperatures, in agreement with the re-entrant nematic phase observed in experiments.

1. Introduction

Liquid crystal polymers (LCPs) combine the functionality of the conventional LCs with the facile processing advantages of polymers, and have been the subject of study in both industrial and academic research.[1−3] To form LCPs, the LC moiety (also called "mesogenic group") can either be incorporated directly into the chain backbone (main-chain LCPs) or be connected to the backbone as a pendant group through a flexible spacer. The latter category, side-chain liquid crystal polymers (SCLCPs), is further divided into side-on SCLCPs and end-on SCLCPs depending on the geometric relationship between the LC side groups and the polymer backbone;[4] see Figure 1. Unlike the main-chain liquid crystal polymers (MCLCPs), the flexibility of the SCLCP backbone is largely maintained. A variety of potential applications for SCLCPs have been considered, such as optical data storage, optically nonlinear media, LC elastomers, separation membranes for complex molecules, etc.[4−6]

In the SCLCPs, there is a competition between the long-range orientational order imparted by their LC character and the tendency to maximize the conformational entropy common to all chain systems. The conformation of the chain backbone is coupled with the nematic ordering to accommodate the orientation of the LC side groups. During the last 20 years, extensive experimental studies have been conducted to determine the conformation of the SCLCPs in the nematic phase.[7−14] Neutron scattering experiments on SCLCP melts,[7−11] reported by Cotton et al., demonstrated that the chain anisotropy is closely related to the local architecture of the attachment. The side-on SCLCPs adopt a highly prolate ellipsoidal conformation in the nematic phase. The chain backbones can be even totally extended as a cylinder under certain conditions.[8] In contrast, the end-on SCLCPs have mild anisotropy and can be either prolate or oblate ellipsoids.[7,11] Kornfield et al. showed that the end-on SCLCPs have a distorted coil conformation by fitting the scattering data with a modified Debye function.[13] Cotton et al. also reported that the end-on SCLCPs can undergo an inversion of the chain anisotropy from a high-temperature nematic phase, in which chain backbone has an oblate shape, to a re-entrant nematic phase where a prolate shape is observed.[10] The conformational transitions of the SCLCPs are illustrated in Figure 1. On the other hand, experimental studies, reviewed by Finkelmann and Rehage, showed that the conformation of the polymer chain backbone also has influence on the nematic ordering of the attached LC molecules.[15,16] Both the transition temperature and the nematic order parameter are found to be affected by the architecture of the attachment, the length of the spacer, the flexibility of the backbone and the graft density of the LC side groups.[15−18]

Theoretically, efforts have also been made to understand the complex phase and conformational behaviors of the LCPs since the pioneering contributions from Onsager and Flory.[19−37] The theories about the MCLCPs have been extensively developed based on the worm-like chain model,[21,22,26−30] where the nematic interaction is usually described by a Maier−Saupe-type pseudopotential.[38] The mean-field equations can either be

*Corresponding author. E-mail: zgw@caltech.edu.

 Published on Web 11/16/2010

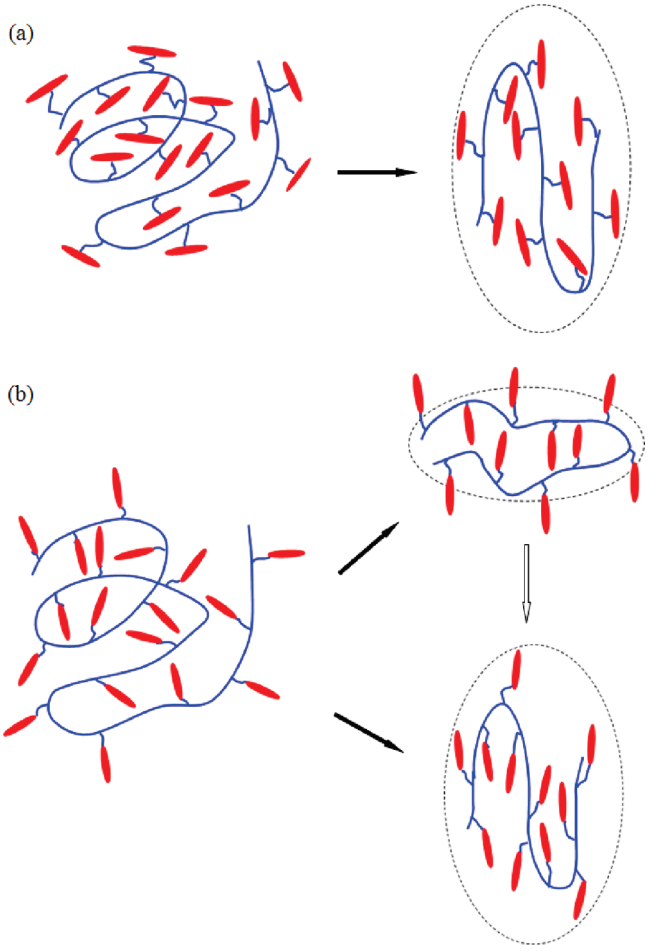

Figure 1. Conformation transitions for side-on (a) and end-on (b) SCLCPs. The solid arrows indicate transitions accompanying the isotropic to nematic transition, whereas the hollow (vertical) arrow represents the shape transition in the nematic phase.

analytically solved by expanding the order parameters around the uniform isotropic state[28] or be numerically solved by using the spheroidal functions.[22,30] It has been found that the competition between the rotational entropy and conformational entropy of the chain segments leads to two important effects: weakening of the nematic ordering at small length scale and hairpin defects at large length scale.[3,22]

In comparison to the MCLCPs, there are fewer theoretical studies on the SCLCP systems. A key issue lies in how to properly describe the coupling between the LC side groups and the chain backbone. Brochard,[34] and subsequently Kyu et al,[35,36] proposed a phenomenological model by combing the Flory–Huggins free energy of mixing and Maier–Saupe free energy of nematic interaction to describe the phase behavior of SCLCPs solutions and blends. The chain backbone in these studies were assumed to be completely decoupled from the LC side groups, which in some sense missed an essential feature of the SCLCPs. By using the worm-like chain model, Carri and Muthukumar[37] studied the chain statistics of side-chain and main-chain LCPs in an ordered anisotropic environment. A parameter was introduced at a mean-field level to describe the coupling between the chain segment and its nematic surroundings. However, this one-parameter model does not explain the complex conformational change of the SCLCPs, especially in the case of the end-on architecture. The most accepted model for the end-on SCLCPs was one by Warner and co-workers.[23,24] They modified their previous worm-like chain model for MCLCPs by considering both the nematic interactions and the effect of chemical attachment between the chain segments and the LC side groups (termed the hinge effect by these authors). The geometry of the molecules and the graft density of the side groups were also taken into account. The competition between different interactions involved in this model was shown to give rise to three types of nematic phases. However, the local hinge effect due to the coupling between a backbone segment and the pendent LC group attached to it was incorporated in that work as a coupling between the backbone orientation and the *global* nematic order parameter. With this prescription, the coupling would vanish in the isotropic state, whereas in reality this coupling should persist irrespective of whether the LC groups orders macroscopically. To date, there is no theoretical work that properly describes the coupling in the SCLCPs and provides a unified treatment of both side-on and end-on attachments.

The coupling between the chain backbone and the LC side groups is the key feature in determining the chain statistics and phase behavior in the SCLCPs systems. It is therefore crucial that this coupling be properly accounted for in a theoretical model. In this article, we propose such a model for the SCLCPs and study the phase behavior and chain conformation. Specifically, we model the coupling between the backbone bond and the LC side groups by two types of terms, one in which the backbone is coupled to the local nematic order parameter, and the other in which the backbone is coupled to its pendant LC group. We call the first type the global coupling term in the sense that the local nematic order parameter is due to orientational order of any LC groups (including LC groups from distance part on the backbone of the same chain as well as LC groups from other chains) that are in the spatial vicinity of the backbone. We call the second type the local coupling term because it represents the direct coupling of the backbone with its own pendant LC group through the spacer. The local coupling term will be assumed to be of the form $u_C(\mathbf{P}_i \cdot \mathbf{q}_i)^2$, where $\mathbf{p}_i$ and $\mathbf{q}_i$ are, respectively, the unit vector for the orientation of the ith backbone bond and that of the pendant LC group attached to it and u_C is a coupling constant with $u_C > 0$ representing side-on attachment and $u_C < 0$ representing end-on attachment. In the next section, we present the model and develop the mean-field (self-consistent-field) equations using standard field-theoretical techniques. In section 3, we use our model to systematically investigate the isotropic–nematic phase transition and the corresponding change of the chain conformation, focusing in particular on the effect of the local coupling and its interplay with the global coupling. The conformational change of the chain backbone caused by varying the LC graft density is also studied. We furthermore connect our model to the structure factor that can be directly measured by scattering experiments. Finally, we discuss possible extensions of the current model and end with a brief conclusion in section 4.

2. Model and Theory

2.1. Model for a SCLCP Melt. We consider an incompressible melt of n_P monodispersed polymer chains in a volume V. In order to focus on the effects of the side-chain liquid-crystal groups, in this work we take the chain backbone to be globally flexible with, however, local rigidity envisioned to arise from the segments that make up the backbone. We thus describe the polymer backbone as a freely jointed chain with $m \cdot N$ chain segments of length b. The chain backbone is assumed to consist of N repeating sections each containing m segments. Each of the repeating sections is grafted with a LC side group. Thus, the structural parameter m reflects the grafting density of the LC side groups, i.e., the grafting

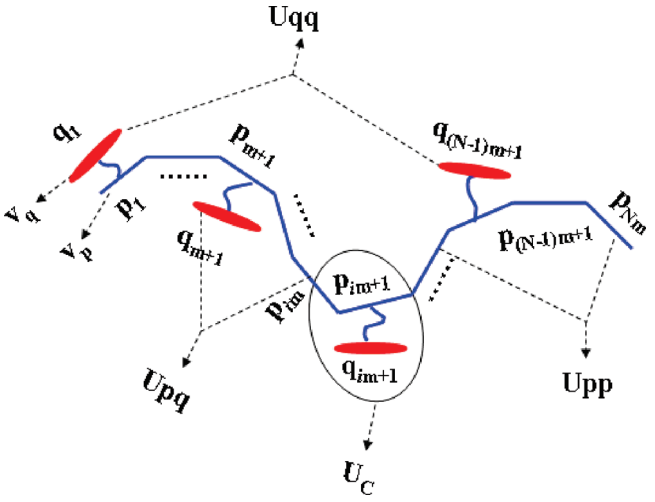

Figure 2. Freely joint chain model for SCLCPs.

density decreases as m increases. To be concrete, we assume that the LC side groups are attached to the first segment in each repeating section. The position and conformation of the α-th polymer chain is described by the position of one of its chain ends, $\mathbf{R}_{\alpha,0}$, and the orientation vectors of all segments. The orientation of the LC-attached chain segment is denoted by a unit vector, $\mathbf{p}_{\alpha,(i\text{-}1)m+1}$, where the subscript indicates it is in the ith repeating section (i = 1, 2, ..., N) of the α-th chain. Similarly, we denote the orientation of the LC side group attached to this chain segment by another unit vector, $\mathbf{q}_{\alpha,(i\text{-}1)m+1}$. The orientation of a chain segment with no LC group attachment (henceforth termed LC-free segment for brevity) is denoted by $\mathbf{p}_{\alpha,(i\text{-}1)m+j}$, with j = 2, 3, ..., m. In addition, the volumes of each chain segment and LC side group are denoted by v_p and v_q, respectively. For simplicity, we neglect the volume occupied by the spacer between the attached segment and side group. (Alternatively, one can interpret $v_q$as including the volume of the spacer at a coarse-grained level.) The effect of the spacer is implicitly included in this model through the local coupling term introduced later. The physical picture of our idealized SCLCPs is illustrated in Figure 2.

We begin by defining the microscopic field operators to characterize the local orientation order of the system:

Nematic orientation operator for the LC-attached chain segments:

$$\widehat{\mathbf{S}}_p(\mathbf{r}) = v_p \sum_{\alpha=1}^{n_P} \sum_{i=1}^{N} \delta[\mathbf{r} - \mathbf{r}_{\alpha,(i-1)m+1}] \left[\mathbf{p}_{\alpha,(i-1)m+1}\mathbf{p}_{\alpha,(i-1)m+1} - \frac{1}{3}\mathbf{I}\right] \tag{1a}$$

where

$$\mathbf{r}_{\alpha,(i-1)m+1} = \mathbf{R}_{\alpha,0} + b \sum_{j=1}^{(i-1)m} \mathbf{p}_{\alpha,j} + \frac{1}{2} b \mathbf{p}_{\alpha,(i-1)m+1}$$

Nematic orientation operator for the LC-free chain segments:

$$\widehat{\mathbf{S}}_{p^*}(\mathbf{r}) = v_p \sum_{\alpha=1}^{n_P} \sum_{i=1}^{N} \sum_{j=2}^{m} \delta[\mathbf{r} - \mathbf{r}_{\alpha,(i-1)m+j}] \left[\mathbf{p}_{\alpha,(i-1)m+j}\mathbf{p}_{\alpha,(i-1)m+j} - \frac{1}{3}\mathbf{I}\right] \tag{1b}$$

where

$$\mathbf{r}_{\alpha,(i-1)m+j} = \mathbf{R}_{\alpha,0} + b \sum_{k=1}^{(i-1)m+j-1} \mathbf{p}_{\alpha,k} + \frac{1}{2} b \mathbf{p}_{\alpha,(i-1)m+j}$$

Nematic orientation operator for the LC side groups:

$$\widehat{\mathbf{S}}_q(\mathbf{r}) = v_q \sum_{\alpha=1}^{n_P} \sum_{i=1}^{N} \delta[\mathbf{r} - \mathbf{r}_{\alpha,(i-1)m+1}] \left[\mathbf{q}_{\alpha,(i-1)m+1}\mathbf{q}_{\alpha,(i-1)m+1} - \frac{1}{3}\mathbf{I}\right] \tag{1c}$$

In eqs 1a and 1b, the contribution from a chain segment at position $\mathbf{r}$ is assumed to come from its middle point. The slight difference in position between the attached chain segment and the LC side group is neglected at the coarse-grained level we are working at. We model the interactions in the system by local two-body pseudopotential and write the Hamiltonian of our system as follows:

$$\begin{aligned} H = & -\frac{U_{pp}}{2}\int d\mathbf{r}\, \widehat{\mathbf{S}}_p(\mathbf{r}) : \widehat{\mathbf{S}}_p(\mathbf{r}) - \frac{U_{p^*p^*}}{2}\int d\mathbf{r}\, \widehat{\mathbf{S}}_{p^*}(\mathbf{r}) \\ & : \widehat{\mathbf{S}}_{p^*}(\mathbf{r}) - \frac{U_{qq}}{2}\int d\mathbf{r}\, \widehat{\mathbf{S}}_q(\mathbf{r}) : \widehat{\mathbf{S}}_q(\mathbf{r}) - U_{pp^*}\int d\mathbf{r}\, \widehat{\mathbf{S}}_p(\mathbf{r}) \\ & : \widehat{\mathbf{S}}_{p^*}(\mathbf{r}) - U_{pq}\int d\mathbf{r}\, \widehat{\mathbf{S}}_p(\mathbf{r}) : \widehat{\mathbf{S}}_q(\mathbf{r}) - U_{p^*q}\int d\mathbf{r}\, \widehat{\mathbf{S}}_{p^*}(\mathbf{r}) \\ & : \widehat{\mathbf{S}}_q(\mathbf{r}) + \sum_{\alpha=1}^{n_P} g_C(\{\mathbf{p}_{\alpha,i}, \mathbf{q}_{\alpha,i}\}) \end{aligned} \tag{2}$$

The first three terms in the Hamiltonian (eq 2) are, respectively, the nematic interactions between the LC-attached segments, between the LC-free segments and between the LC side groups. The second three terms in eq 2 are the nematic cross-interactions between any two of the above three moieties. All these nematic interactions are treated in a coarse-grained approach, and taken to be of the Maier−Saupe type.[38] They represent the average orientational interaction of a moiety (chain segment or LC group) with its surroundings. The six nematic interaction parameters, $U_{\kappa,\kappa'}(\kappa, \kappa' = p, p^*$, and $q)$, which have units of energy per volume, include both the entropic (Flory−Onsager) and energetic (van der Waals) forces. They provide the drive toward parallel order of the interacting groups. We distinguish between the nematic interaction parameters related to the LC-attached and the LC-free chain segments in order to allow the differences in chemical structure between them.

The last term in eq 2 accounts for the local coupling between the LC side group and the chain segment it is attached to. While the total effects of side-chain LC grafting may be multifold, the main effect we wish to capture in this work is the preferred orientation of the LC side group with respect to the orientation of the particular chain segment: i.e., the side-on attachment prefers a parallel orientation, while the end-on attachment prefers a perpendicular orientation. We model this effect at a phenomenological level by a simple quadratic term of the following form:

$$g_C(\{\mathbf{p}_{\alpha,i}, \mathbf{q}_{\alpha,i}\}) = -\sum_{i=1}^{N} u_C(\mathbf{p}_{\alpha,(i-1)m+1} \cdot \mathbf{q}_{\alpha,(i-1)m+1})^2 \tag{3}$$

where u_C is the coupling parameter, the magnitude of which determines the strength (tightness) of the coupling (which can be controlled by the spacer length, for example), while its sign dictates whether parallel or perpendicular orientation is

energetically favored: $u_C > 0$ represents the case of side-on SCLCPs where parallel alignment between $\mathbf{p}_{(i\text{-}1)m+1}$ and $\mathbf{q}_{(i\text{-}1)m+1}$ is energetically preferable and $u_C < 0$ corresponds to the case of end-on SCLCPs where these two vectors prefer to be perpendicular to each other. In this work, we assume the local coupling effect to be of a "self-coupling type", that is, we only consider the LC side group (see Figure 2) and the backbone segment it is attached to is taken into account; couplings between the LC side group and adjacent chain segments are neglected.

The form of the coupling between the LC side group and its attaching backbone segment, eq 3, represents the key difference between our work and the work of Wang and Warner.[23] In their work, the coupling effect is treated as an interaction between the chain vector and the average nematic order parameter; the coupling would vanish in the isotropic phase. In our model, the coupling is between the instantaneous values of the two vectors; it persists even in the isotropic phase, which is more realistic in capturing the correct physics.

2.2. Self-Consistent Field Theory. As a many-body problem, the model cannot be solved exactly. In this work, we use the self-consistent field theory, which is a mean-field approximation. The self-consistent field theory can be derived in several ways. A common strategy is to map the interacting multichain problem into a problem of a single chain in a fluctuating field by some identity transformation involving functional integration over the fluctuating field(s). The mean-field (self-consistent field) approximation then replaces the functional integration by the saddle point method. We refer interested readers to the relevant literatures[30,33,39,40] for more detailed derivation. For the case of a homogeneous liquid, as is the focus here, the self-consistent field theory ultimately reduces to the computation of the partition function of a single chain in spatially uniform nematic fields:

$$\begin{aligned} Q_p = \prod_{i=1}^{N}\prod_{j=1}^{m}\Big(\int \mathrm{d}\mathbf{p}_{(i-1)m+j}\Big)\int \mathrm{d}\mathbf{q}_{(i-1)m+j}\Big)\exp\Bigg\{\sum_{i=1}^{N}\beta v_p\big(U_{pp}\mathbf{S}_p \\ + U_{pp^*}\mathbf{S}_{p^*} + U_{pq}\mathbf{S}_q\big) : \left(\mathbf{p}_{(i-1)m+1}\mathbf{p}_{(i-1)m+1} - \frac{1}{3}\mathbf{I}\right) \\ + \sum_{i=1}^{N}\sum_{j=2}^{m}\beta v_p\big(U_{pp^*}\mathbf{S}_p + U_{p^*p^*}\mathbf{S}_{p^*} + U_{p^*q}\mathbf{S}_q\big) : \left(\mathbf{p}_{(i-1)m+j}\mathbf{p}_{(i-1)m+j} - \frac{1}{3}\mathbf{I}\right) \\ + \sum_{i=1}^{N}\beta v_q\big(U_{pq}\mathbf{S}_p + U_{p^*q}\mathbf{S}_{p^*} + U_{qq}\mathbf{S}_q\big) : \left(\mathbf{q}_{(i-1)m+1}\mathbf{q}_{(i-1)m+1} - \frac{1}{3}\mathbf{I}\right) \\ + \sum_{i=1}^{N}\beta u_C\big(\mathbf{p}_{(i-1)m+1}\cdot\mathbf{q}_{(i-1)m+1}\big)^2\Bigg\} \end{aligned} \tag{4}$$

where $\mathbf{S}_k$ ($\kappa = p$, p^*, and q) are the tensorial nematic order parameters corresponding to the nematic orientational operators. The equilibrium values of $\mathbf{S}_k$ are given by

$$\mathbf{S}_p = \frac{n_P v_p}{V}\Big\langle\sum_{i=1}^{N}\big(\mathbf{p}_{(i-1)m+1}\mathbf{p}_{(i-1)m+1} - \frac{1}{3}\mathbf{I}\big)\Big\rangle \tag{5a}$$

$$\mathbf{S}_{p^*} = \frac{n_P v_p}{V}\Big\langle\sum_{i=1}^{N}\sum_{j=2}^{m}\big(\mathbf{p}_{(i-1)m+j}\mathbf{p}_{(i-1)m+j} - \frac{1}{3}\mathbf{I}\big)\Big\rangle \tag{5b}$$

$$\mathbf{S}_q = \frac{n_P v_q}{V}\Big\langle\sum_{i=1}^{N}\big(\mathbf{q}_{(i-1)m+1}\mathbf{q}_{(i-1)m+1} - \frac{1}{3}\mathbf{I}\big)\Big\rangle \tag{5c}$$

where the ensemble averages are taken based on the Boltzmann factor appearing in eq 4. For uniaxial order, we take the nematic director to be aligned in the z-direction. Thus, the three tensorial nematic order parameters $\mathbf{S}_k$ are diagonal and traceless. Their corresponding scalar forms of nematic order parameter, s_κ, are defined by normalizing the $\hat{z}\hat{z}$ components of $\mathbf{S}_k$ with respect to the volume fractions. They are given by

$$s_p = \frac{3}{2}\frac{\mathbf{S}_{p,zz}}{\varphi_p} = \frac{1}{N}\Big\langle\sum_{i=1}^{N}P_2(\cos\theta_{p,(i-1)m+1})\Big\rangle \tag{6a}$$

$$s_p{}^* = \frac{3}{2}\frac{\mathbf{S}_{p^*,zz}}{\varphi_{p^*}} = \frac{1}{N(m-1)}\Big\langle\sum_{i=1}^{N}\sum_{j=2}^{m}P_2(\cos\theta_{p,(i-1)m+j})\Big\rangle \tag{6b}$$

$$s_q = \frac{3}{2}\frac{\mathbf{S}_{q,zz}}{\varphi_q} = \frac{1}{N}\Big\langle\sum_{i=1}^{N}P_2(\cos\theta_{q,(i-1)m+1})\Big\rangle \tag{6c}$$

where $\varphi_p = n_p N v_p/V$, $\varphi_{p^*} = n_p N(m-1)v_p/V$ and $\varphi_p = n_p N v_p/V$ are, respectively, the volume fractions of the LC-attached chain segment, the LC-free chain segment, and the LC side group. $P_2(x)$ is the second order Legendre polynomial

$$P_2(x) = \frac{3}{2}x^2 - \frac{1}{2}$$

The normalization of $\mathbf{S}_k$ is introduced to avoid the nematic order parameters vanishing in the limit of zero volume fraction. The prefactor, $^3/_2$, in eq 6 is used so that the order parameters defined here conform to the form in the Maier−Saupe theory.[33]

If the main chain backbone is globally flexible, it is reasonable to assume that the nematic self-interactions between chain segments are much weaker than other nematic interactions (i.e., U_{pp}, U_{pp^*}, and $U_{p^*p^*}$ are negligible compared to U_{qq}, U_{pq}, and U_{p^*q}). In addition, the single chain partition function in eq 4 is further decoupled into the partition function of one repeating section Q_S, i.e. $Q_p = (Q_S)^N$, based on the "self-coupling" form for the local coupling, eq 3. Thus, the resulting Q_S can be written as:

$$\begin{aligned} Q_S = \int \mathrm{d}\mathbf{p}\int \mathrm{d}\mathbf{q}\exp\{\beta[\varphi_p\varphi_q u_{pq}s_q P_2(\cos\theta_p) \\ + (\varphi_p\varphi_q u_{pq}s_p + \varphi_{p^*}\varphi_q u_{p^*q}s_{p^*} + \varphi_q{}^2 u_{qq}s_q)P_2(\cos\theta_q) \\ + u_C(\mathbf{p}\cdot\mathbf{q})^2]\}\{\int \mathrm{d}\mathbf{p}^*\exp[\beta\varphi_{p^*}\varphi_q u_{p^*q}s_q P_2(\cos\theta_{p^*})/(m-1)]\}^{m-1} \end{aligned} \tag{7}$$

where $\mathbf{p}$, $\mathbf{q}$, and $\mathbf{p}^*$ are the unit vectors denoting the LC-attached segment, the LC-free segment, and the LC side group, respectively. $u_{\kappa,\kappa'}$ ($\kappa,\kappa' = p$, p^*, and q) are defined by normalizing $U_{\kappa,\kappa'}$ with respect to the density of the repeating section, i.e. $u_{kk'} = (2/3)U_{kk'}V/(Nn_P)$. We introduce another structural parameter γ to reflect the volume ratio of the LC side group and the chain segment, as $\gamma = v_q/v_p$. The volume fractions of the three components are then expressed by the two structural parameters m and γ, as $\varphi_p = 1/(m+\gamma)$, $\varphi_{p^*} = (m-1)/(m+\gamma)$, and $\varphi_q = \gamma/(m+\gamma)$. Therefore, the partition functions are determined by the nematic interaction parameters $u_{\kappa,\kappa'}$, the local coupling parameter u_C, and the structural parameters m, γ. The resulting order parameters s_κ are then the ensemble averages taken based on eq 7:

$$s_\kappa = \Big\langle P_2(\cos\theta_\kappa)\Big\rangle \tag{8}$$

Equations 7 and 8 form a complete set of self-consistent equations which can be solved numerically in an iterative way. Whether the nematic or the isotropic phase is physically more stable can be determined through comparing their corresponding values of free energy. With the factorization

of the single-chain partition function into product of each repeating unit, the free energy of a repeating section can be easily evaluated from the saddle-point value of the order parameters as

$$\beta F = \beta\left(\frac{1}{2}\varphi_q{}^2 u_{qq} s_q{}^2 + \varphi_p \varphi_q u_{pq} s_p s_q + \varphi_{p^*} \varphi_q u_{p^*q} s_{p^*} s_q\right) - \ln Q_S \tag{9}$$

For simplicity, all the parameters, in this paper, are assumed to be temperature-independent. However, the temperature dependence of parameters can be easily included in the model, which will give rise to richer phase behaviors.

2.4. Chain Statistics. The equilibrium value of s_q is a measure of the alignment between the LC side groups and the nematic axis. As in the Maier−Saupe theory, s_q can range from 0 (completely random orientation) to 1 (fully parallel alignment) in our model. On the other hand, s_p and s_{p^*} measure the orientation of the LC-attached chain segments and the LC-free segments with respect to the nematic axis, respectively. Both s_p and s_{p^*} range from −0.5 to 1, with a positive value corresponding to parallel alignment and a negative value corresponding to perpendicular alignment. The orientation of a single chain segment can directly affect the conformation of whole polymer chain. For the freely jointed chain with $m \cdot N$ segments (i.e., $m \cdot (N + 1)$ monomer units), the mean square end-to-end distance vector in the direction parallel to the nematic axis, $\langle R_\parallel{}^2 \rangle$, is given by:[41]

$$\left\langle R_\parallel{}^2 \right\rangle = \left\langle R_Z{}^2 \right\rangle = \frac{1}{(mN+1)^2} \sum_{i=0}^{mN} \sum_{j=i}^{mN} \left\langle (Z_j - Z_i)^2 \right\rangle$$

$$= \frac{1}{(mN+1)^2} \sum_{i=0}^{mN} \sum_{j=i}^{mN} \sum_{k=i+1}^{j} \left\langle (\cos\theta_k b_p)^2 \right\rangle \tag{10}$$

where Z_i and Z_j are the coordinates of monomer i and j in z direction, respectively; and $\cos\theta_k\, b_p$ is the z component of the vector denoting the k-th chain segment. For very long polymer chain,

$$\left\langle R_\parallel{}^2 \right\rangle \cong \frac{1}{(mN+1)^2} \sum_{i=0}^{mN} \sum_{j=i}^{mN} \left(\frac{1}{m} \left\langle \cos^2\theta_p \right\rangle + \frac{m-1}{m} \left\langle \cos^2\theta_{p^*} \right\rangle \right) |j-i| b_p{}^2 = \left\langle R_g{}^2 \right\rangle \left(\frac{1}{3} + \frac{2}{3}\bar{s}_p \right) \tag{11}$$

where $\bar{s}_p = s_p/m + (m - 1)s_{p^*}/m$ is the order parameter representing the average orientation of all the chain segments. $\langle R_g{}^2 \rangle$ is the mean square radius of gyration for a freely joint chain in the isotropic phase, i.e., $\langle R_g{}^2 \rangle = mNb_p{}^2/6$. In addition, the mean square end-to-end distance in the perpendicular direction $\langle R_\perp{}^2 \rangle$ can be similarly expressed as

$$\left\langle R_\perp{}^2 \right\rangle = \left\langle R_g{}^2 \right\rangle \left(\frac{1}{3} - \frac{1}{3}\bar{s}_p \right) \tag{12}$$

The anisotropic ratio is given by:

$$\frac{R_{||}}{R_\perp} = \sqrt{\frac{\left\langle R_\parallel{}^2 \right\rangle}{\left\langle R_\perp{}^2 \right\rangle}} = \sqrt{\frac{1 + 2\bar{s}_p}{1 - \bar{s}_p}}$$

$$= \sqrt{\frac{m(1 + 2s_{p^*}) + 2(s_p - s_{p^*})}{m(1 - s_{p^*}) - (s_p - s_{p^*})}} \tag{13}$$

which is determined by s_p, s_{p^*} and the graft density. The deviation of the anisotropic ratio from unity indicates the extent of the chain distortion from spherical, with $R_\parallel/R_\perp > 1$ representing a prolate conformation and $R_\parallel/R_\perp < 1$ representing an oblate conformation.

3. Results and Discussion

In the last section, we have constructed a model that unifies both the cases of side-on and end-on SCLCPs. The equilibrium order parameters are determined by the nematic interactions, the local coupling and the structural parameters. In the model, the nematic field (reflected by the alignment of the LC side groups) and the chain conformation (related to the orientation of chain segments) interplay with each other through two effects: the nematic cross-interaction (henceforth referred to as the "global coupling effect") and the local coupling effect. In the following, we investigate how the isotropic−nematic phase transition and the chain conformation are affected by these two coupling effects.

3.1. The Coupling Effects on Chain Conformation and Phase Transition. The global coupling arises from the local rigidity and/or anisotropy of the chain backbone segments, which is reflected by the Kuhn segment in the freely joint chain model. On the basis of the idea of Maier−Saupe theory, there should be some nematic interaction between the "rod-like" LC side groups and the "stick-like" Kuhn segments. This coupling is realized through the global variables: s_p, s_{p^*}, and s_q. From the mean-field perspective, a change in the nematic order will affect the average orientation of the chain segments, and vice versa. The coupling only exists in the nematic state. In contrast, the local coupling owes its origin to the chemical linkage between the polymer chain and the LC side groups. Its strength depends on the nature of the spacer, such as the chemical structure, the length, the odd−even effect, etc. Within one attached pair, the LC side group and the chain segment need to accommodate their orientation to each other according to the architecture of attachment (side-on or end-on). In addition, the orientation of adjacent chain segments may become restricted due to the excluded volume effect of the grafted LC moieties (this will be discussed further). The local coupling persists even in the isotropic phase. Because of their different nature, these two coupling effects play different roles on the chain conformation and the phase transition: the effects of the global coupling are more direct, while those of the local coupling are more indirect (but not any less important!). Distinguishing between these two coupling effects and properly accounting for them constitutes a key difference between our work and previous studies.

In this subsection, we focus on the coupling effects, and thus set $m = 1$ (i.e., every chain segment is grafted with a LC side group); the influence of the LC grafting density will be discussed in the next subsection. For $m = 1$, the chain conformation is directly related to the orientation of the LC-attached segments, s_p, as shown in eq 13. In the isotropic phase, the global coupling disappears automatically owing to the absence of the nematic order. The local coupling still exists and keeps the chain segments with their attached LC side groups correlated. However, statistically, the average orientation of chain segments is still random (i.e., $s_p = 0$) for lacking long-range order of the LC side groups in the system. Therefore, at the mean-field level, the polymer chain remains an undistorted random coil in the isotropic phase, in agreement with the experimental results.[7]

In the nematic phase, the chain conformation is undistorted when both the global and the local coupling are absent (as in the case of $u_{pq} = 0$ and $u_C = 0$ in Figure 3a. This simple

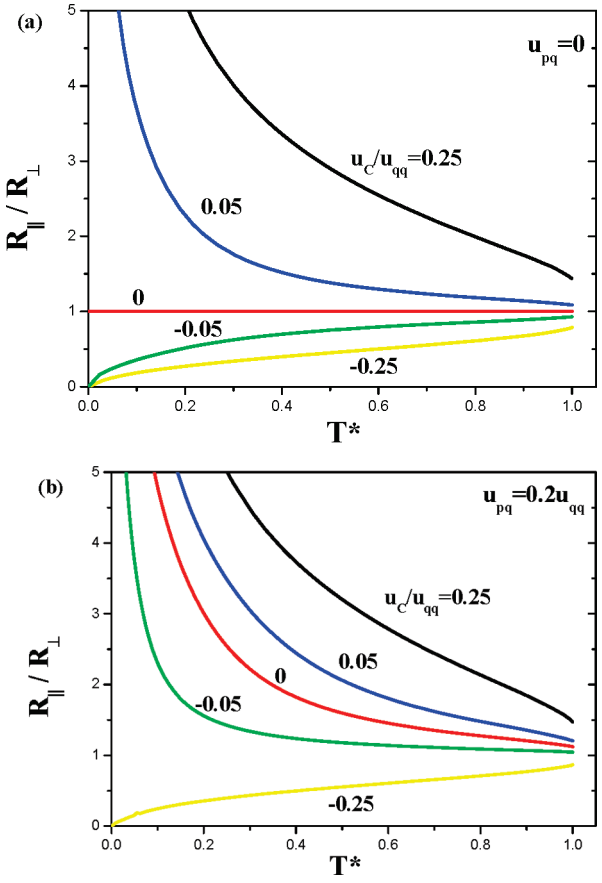

Figure 3. Conformation anisotropy ration $R_\parallel/R_\perp$ as a function of the reduced temperature. $T^* = T/T_C$, where T_C is the corresponding phase transition temperature, which is different for different parameters. Key: (a) $u_{pq} = 0$; (b) $u_{pq} = 0.2u_{qq}$.

case corresponds to the models studied by Brochard[34] and by Kyu et al.[35,36] In the presence of the coupling, the chain segments become oriented as soon as the nematic order appears (i.e., $T^* = T/T_C < 1$), and the conformation of the polymer chain becomes anisotropic. We first investigate the effect of the local coupling by turning off the global coupling (i.e., $u_{pq} = 0$). In this case, the chain segment tends to be parallel to the corresponding LC side group for the side-on attachment (i.e., $u_C > 0$) and perpendicular for the end-on attachment (i.e., $u_C < 0$). In Figure 3a, we show the changes of the anisotropic ratio with respect to the reduced temperature at different values of u_C. Clearly, without the global coupling, the side-on SCLCPs adopt a prolate conformation whereas the end-on SCLCPs adopt an oblate conformation in the nematic phase. The degree of anisotropy increases with increasing the coupling or decreasing the temperature.

Small-angle neutron scattering (SANS) experiments conducted by Cotton et al.[7,8,11] show that side-on SCLCPs always adopt a prolate ellipsoid conformation in the nematic phase. However, end-on SCLCPs can be either prolate or oblate ellipsoids.[7] This is not captured by theoretical results shown in Figure 3a, which suggests that local coupling alone is not sufficient to explain all the conformational changes of the SCLCPs observed in experiments, and the effect of the global coupling should also be taken into account (as shown in Figure 3b). Because of the global coupling, each chain segment tends to be aligned parallel to the nematic field. It should be noted that, even without the local coupling (as the case of $u_C = 0$ in Figure 3b), the chain conformation will be prolate in the nematic phase. $u_C = 0$ implies that the LC side groups are locally decoupled from the chain backbone, which can be realized through a very long spacer. This kind of SCLCP melt is in essence similar to a homogeneous solution of non-LC polymers in LC solvent. Dubault et al.[42] found experimentally that the conformation of non-LC polymers in LC solvent is not isotropic but slightly prolate; this is in agreement with our theoretical consideration.

When global and local couplings both exist, their combined effects are quite different for the side-on and the end-on SCLCPs. For the case of side-on SCLCPs, the local hinge effect makes each chain segment align parallel to its attached LC side group with fluctuations around the nematic director. Statistically, the local coupling provides the same effect as the global coupling that enforces the parallel alignment of the chain segments with the nematic field. The two coupling effects act cooperatively, and thus, the prolate anisotropy of the chain conformation is enhanced in the side-on SCLCPs. Parts a and b of Figure 3 show that, if $u_C > 0$, $R_\parallel/R_\perp$ increases as either u_C or u_{pq} increases. In contrast, for the case of end-on SCLCPs, the local hinge effect tends to have the chain segments aligned perpendicularly to the nematic field, which competes with the global coupling that favors a parallel alignment. Thus, whether the polymer chains adopt a prolate or an oblate conformation depends on the relative strengths of these two coupling effects. By weakening the local coupling (e.g., increasing the spacer length), the oblate conformation for the end-on SCLCPs, may turn into the prolate. This effect is shown in Figure 3b: $R_\parallel/R_\perp$ shifts upward above 1 when u_C/u_{qq} changes from -0.25 to -0.05. The same conformational change is also predicted by strengthening the global coupling (e.g., increasing the rigidity of the chain backbone segments). It can be seen from parts a and b of Figure 3 that, for the case of $u_C/u_{qq} = -0.05$, the previous oblate conformation changes to prolate when u_{pq} increases from 0 to 0.2. This result is consistent with the experimental observation that the end-on SCLCPs with more flexible polymethylsiloxane backbone tend to form an oblate ellipsoid whereas the SCLCPs with more rigid polymethacrylate backbone tend to be prolate.[12] Therefore, the relation between the effects of the global and the local coupling on chain conformation is competitive in the end-on SCLCPs instead of cooperative as in the side-on SCLCPs. Our theoretical results also qualitatively explain the experimental observation by Cotton et al. that the end-on SCLCPs usually exhibit milder anisotropy than the side-on SCLCPs.[7]

Finkelmann and Rehage[16] point out that the transition temperature and the nematic order parameter of the SCLCPs are different from the corresponding small LC molecules. The polymer segments affect the nematic order and transition through two effects: dilution of the mesogen concentration and coupling, both local and global. In the absence of the global coupling and bending energy cost between adjacent segments, the orientation of a chain segment cannot propagate to other segments either on the same chain or on different chains. The local coupling merely makes the chains adjust their conformation in accordance with the preferred orientation of the LC side groups. In other words, in the absence of the global coupling, the attachment of the polymer chain to the LC side groups does not contribute to the nematic order of the LC side groups aside from a simple dilution effect. Consequently, the transition temperature, once corrected for the dilution effect, is unaffected by the presence the local coupling;[43] this is shown in the case of $u_{pq} = 0$ in Figure 4. This result also confirms the crucial difference between the global and local coupling effects that have been missed in earlier studies by Wang and Warner.

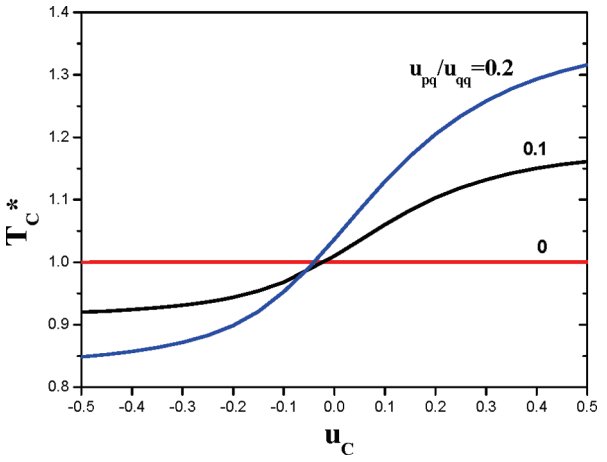

Figure 4. Effect of the coupling parameters on the transition temperature. T_C* is the reduced phase transition temperature scaled as: $T_C^* = T_C/T_{C,0}$, where $T_{C,0}$ is the transition temperature for the totally decoupled case ($u_C = 0$ and $u_{pq} = 0$). $T_{C,0} = \varphi_q^2 u_{qq}/4.53k_\beta$, corrected from the Maier−Saupe theory by the dilution effect.

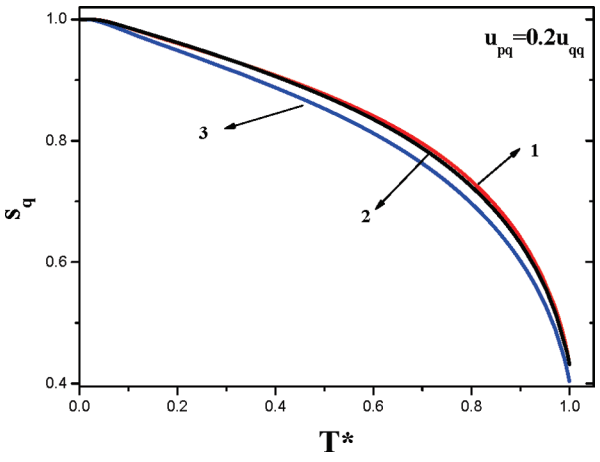

Figure 5. Nematic order parameter s_q as a function of the reduced temperature for $u_{pq} = 0.2u_{qq}$. Lines 1 (red), 2 (black), and 3 (blue) represent the cases of $u_C = 0.25$, 0, and −0.25, respectively.

The global coupling terms directly affects the nematic order and the transition temperature. The mean-field energy associated with the global coupling is $-\varphi_p\varphi_q u_{pq} s_p s_q - \varphi_{p^*}\varphi_q u_{p^*q} s_{p^*} s_q$. For the homopolymer chain backbone, we do not need to distinguish u_{p^*q} from u_{pq}. On the basis of the definition of the structural parameters (the grafting density m and the volume ratio γ) and the order parameter $\bar{s}_p$, the global coupling energy is rewritten as $-m\gamma u_{pq}\bar{s}_p s_q/(m+\gamma)^2$. $\bar{s}_p$ reflects the average orientation of all the chain segments and is directly related to the chain conformation through eq 13 (e.g., $\bar{s}_p > 0 \Rightarrow R_\parallel/R_\perp > 1$). Thus, $R_\parallel/R_\perp > 1$ is energetically preferable, whereas $R_\parallel/R_\perp < 1$ is penalized. From the viewpoint of phase transition, the prolate chain conformation enhances the favorable attraction, resulting in an easier transition to an ordered phase (i.e., increasing the transition temperature). The oblate conformation frustrates the nematic field, and thus decreases the transition temperature. However, without the local coupling term, the effect on the transition temperature is relatively minor. The effect is significantly enhanced by the presence of the local coupling. In Figure 4, we show the combined effect due to both the global and local coupling by plotting the transition temperature as a function of the local coupling parameter for three values of the global coupling parameter. For the case of $u_{pq} = 0$, the transition temperature is independent of the change of u_C as pointed out earlier. But for the cases of $u_{pq} > 0$, T_C* increases monotonously as u_C increases (reflecting the increased tendency of the chain conformation to adopt a prolate shape). The impact of the chain conformation on the nematic field gets stronger when we strengthen the global coupling. Form these results we infer that, for the SCLCPs with certain rigidity on the chain backbone, the transition temperature should increase in the following order: tightly hinged end-on → loosely hinged end-on → locally decoupled → loosely hinged side-on → tightly hinged side-on. Both Finkelmann et al.[16] and Mattoussi et al.[12] observe that transition temperature increases as the spacer length of the end-on SCLCPs increases, which is consistent with our theoretical analysis.

Unlike the transition temperature, the order parameters s_q vs the temperature T* only shows a weak dependence on u_C for the case of $u_{pq} > 0$, as shown in Figure 5. This indicates that the nematic order parameter is mainly determined by the reduced temperature and is not sensitive to the local coupling effect. This phenomenon has also been observed in the experiment of Finkelmann and Rehage[16] when they change the spacer length of the end-on SCLCPs from 3 to 6 CH_2 units. In addition, we can see from Figure 5 that, the value of s_q at transition temperature is lower for the end-on SCLCPs than the decoupled case ($u_C = 0$), which is also in agreement with their experiment data.[16]

3.2. Effects of LC Grafting Density on Chain Anisotropy. In the last subsection, we focused on the differences and interplay between the global and local coupling on the behavior of the SCLCPs by setting $m = 1$, i.e., a LC side group for every chain segment. The LC grafting density, reflected by the structural parameter m, has effect on both the order parameters and the chain statistics as shown in eqs 7 and 13. It is possible in the real polymer system or the polymerization process to have less than one LC side group per Kuhn segment. For $m > 1$, there are $m - 1$ LC-free chain segments for every LC attachment. Therefore, as m increases, the role of the LC-free segments becomes more important in the chain statistics. The global coupling acts on both types of segments whereas the local coupling only affects the LC-attached chain segments. The local effect gets diluted as the fraction of the LC-free segments increases, which changes the relative strengths between the two coupling effects. Below we discuss the effect of the LC grafting density on the chain anisotropy.

As indicated earlier, the global and the local coupling effects act cooperatively to enhance the parallel alignment of the chain segments with the nematic field in the case of side-on SCLCPs. The alignment of the LC-attached segments is more ordered than the LC-free segments because of the reenforcement by the local coupling effect. As m increases, the average order of the chain segments at a certain reduced temperature (i.e., corresponding roughly to the same nematic field) decreases. The resulting chain conformation becomes less prolate. The change of anisotropic ratio at different LC grafting densities is shown in Figure 6a. It can be seen that the prolate anisotropy is greatly reduced as $m$increases from 1 to 2. The reduction becomes less significant when we further decrease the LC graft density (see the curves for $m = 3$ and 4 in Figure 6a).

The m-dependence of the chain conformation is more interesting for the end-on SCLCPs since the two coupling effects are competitive in this case. The orientation of the LC-attached chain segments is determined by the relative strength of the local and global coupling, which prefers the perpendicular and the parallel alignment, respectively.

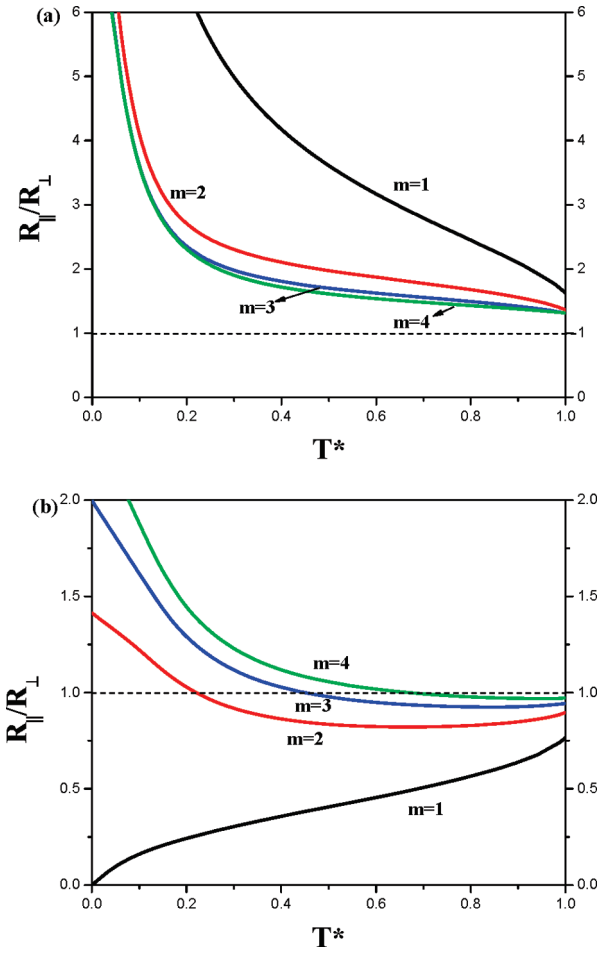

Figure 6. Conformation anisotropic ratio $R_\parallel/R_\perp$ as a function of the reduced temperature for different LC grafting densities, m. Key: (a) side-on SCLCPs with $u_C = 0.5u_{qq}$, $u_{pq} = 0.1u_{qq}$; (b) end-on SCLCPs with $u_{pq} = 0.1u_{qq}$, $u_C = -0.5u_{qq}$. The dashed line represents the isotropic conformation ($R_\parallel/R_\perp = 1$).

On the other hand, the LC-free segments, affected by the global coupling, can only be aligned parallel with the nematic axis. Thus, besides the competition between the two coupling effects, the final chain conformation also depends on the competition between the orientations of the LC-attached and LC-free segments. As m increases, the relative effect of the local coupling on the system is weakened, and the chain conformation gets gradually controlled by the orientation of the LC-free segments. Figure 6b shows the effect of the LC grafting density on the anisotropic ratio for the end-on SCLCPs. The orientation of the LC-attached segments in this system is dominated by the local coupling effect, manifested as the oblate conformation in the fully attached case ($m = 1$). With the increase of m, the oblate conformation, however, becomes less obvious in the temperature range not far below the phase transition. More interestingly, for the systems with $m > 1$, the chain conformation transforms from oblate to prolate at lower temperatures. This conformational transition is due to the fact that as temperature decreases, the LC-free chain segments get more and more oriented parallel to the nematic field, which dominate over the perpendicularly oriented LC-attached segments. As shown in Figure 6b, the conformational transition shift to a higher temperature when m increases.

For the same end-on SCLCPs system, Cotton et al.[10] observed a re-entrant nematic phase appearing at lower temperature comparing to the usual nematic phase and smectic A phase. There is an inversion of the chain anisotropy from the oblate shape in the high temperature nematic phase to the prolate shape in the re-entrant nematic phase. Although we do not consider the smectic A phase in our study, we believe that the same physics as we have elucidated theoretically here is at play in the experimental systems. We note that a similar result was also predicted in Wang and Warner's model.[23] However, they treated the hinge effect via global interactions and did not locally distinguish between the LC-attached and LC-free segments. Thus, in their model, all the chain segments become oriented in the parallel direction in the re-entrant nematic phase, which results in a very strong chain anisotropy. In our model, the effect of the parallel alignment of the LC-free segments on chain conformation is partially counteracted by the perpendicular alignment of the LC-attached segments. Thus, the chain anisotropy in the re-entrant nematic phase predicted by our model is mild, which is in agreement with the experimental data of Cotton et al.

3.3. Structure Factor. Small-angel scattering techniques, such as SANS and SAXS, are the major tools to determining the single chain conformation, because they provide direct measurement on the structure factor.[44] In this subsection, we examine the chain anisotropy in the nematic phase as revealed by the structure factor due to the combined effects of global and local coupling between the chain backbone and the LC side groups.

Similar to the well-known Debye function of flexible non-LC polymers,[41] the structure factor for the anisotropic freely joint chain can be written as:

$$S(q_\parallel, q_\perp) = \frac{2}{[X(q_\parallel, q_\perp)]^2}\left[e^{X(q_\parallel, q_\perp)} - 1 + X(q_\parallel, q_\perp)\right] \quad (14)$$

which shows differences in the parallel and perpendicular directions. $X(q_\parallel,q_\perp)$ is a function of $q_\parallel$ and $q_\perp$ given as:

$$X(q_\parallel, q_\perp) = \langle R_g^2 \rangle \left[q_\parallel^2 \left(1 + \frac{2s_p + 2(m-1)s_{p^*}}{m}\right) + q_\perp^2 \left(1 - \frac{s_p + (m-1)s_{p^*}}{m}\right)\right] \quad (15)$$

When $s_p = s_{p^*} = 0$, $X(q_\parallel,q_\perp)$ reduces to $\langle R_g^2 \rangle q^2$, and thus, $S(q_\parallel,q_\perp)$ reduces to the Debye structure factor.

Figure 7 shows the 2-dimensional patterns of the structure factor for different values of u_C and $\boldsymbol{m}$. The conformational anisotropy is clearly reflected by the asymmetry of the pattern in parallel and perpendicular directions. The local coupling parameter significantly affects the chain conformation. For the case of $m = 1$, the polymer backbone changes from the prolate to the oblate conformation as u_C changes from positive to negative. The effect of u_C on chain conformation becomes less significant in the case of $m = 3$. In addition, the chain conformation is also affected by the LC grafting density, and behaves differently depending on the architecture of the attachment. For the side-on SCLCPs (u_C=0.5), the prolate conformation becomes less pronounced as m increases (cf. Figure 7, parts a and d). For the decoupled SCLCPS ($u_C = 0$), the values of m have no influence on the chain conformation (cf. Figure 7, parts b and e) because the LC-attached and LC-free segments are acted upon by the same global field. For the end-on SCLCPs ($u_C = -0.5$), the chain conformation transforms from oblate to prolate as m increases (cf. Figure 7, parts c and f).

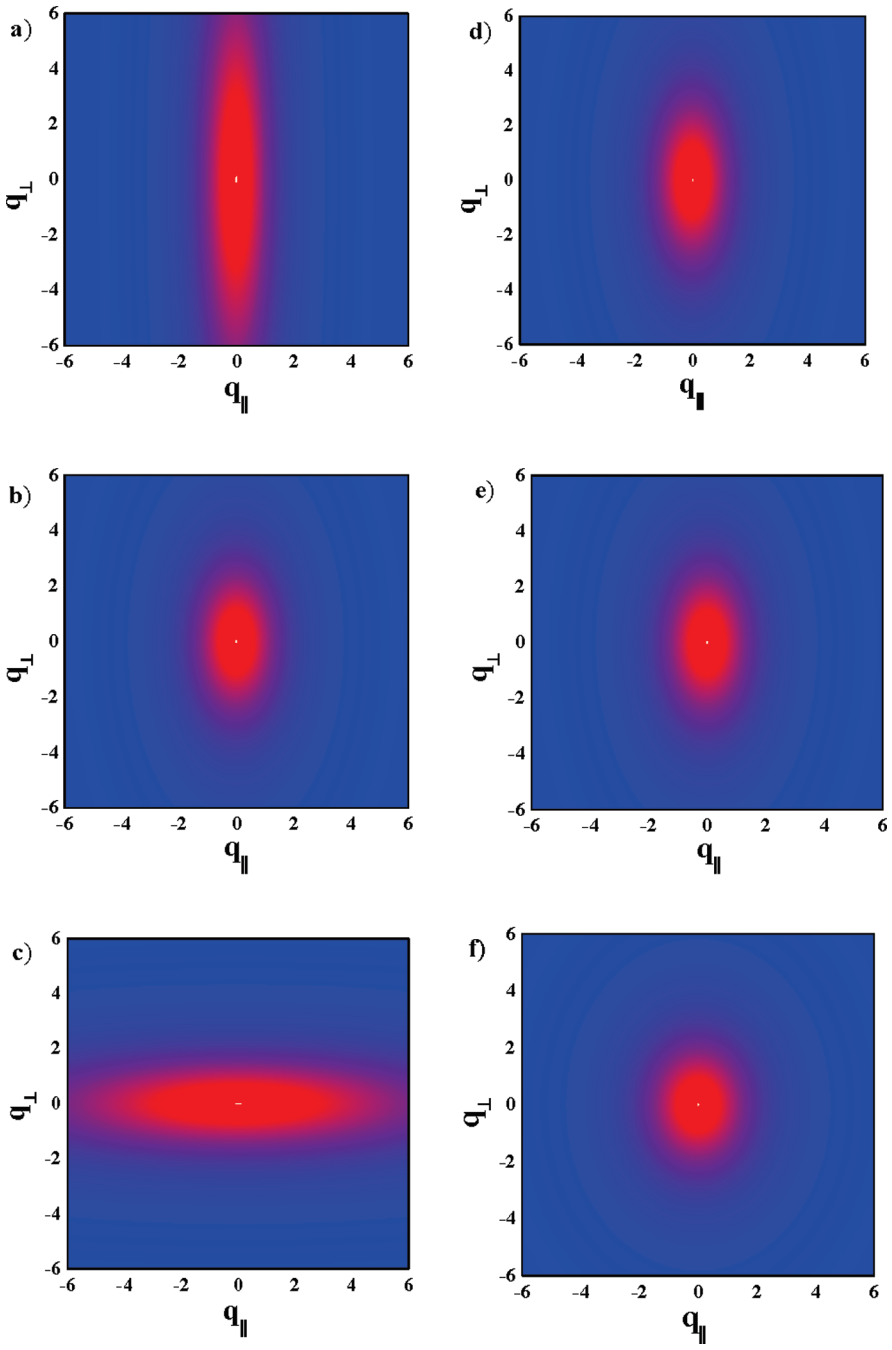

Figure 7. Two-dimensional cross-section of structure factor at $T^* = 0.2$. $q_\parallel$ and $q_\perp$ are given in units of $\langle R_g \rangle^{-1}$. From parts a) to c), $u_{pq} = 0.1u_{qq}$, $m = 1$, $u_C = 0.5u_{qq}$, 0, and $-0.5u_{qq}$, respectively. From parts d) to f), $u_{pq} = 0.1u_{qq}$, $m = 3$, $u_C = 0.5u_{qq}$, 0, and $-0.5u_{qq}$, respectively.

From eq 14, we can define reduced 1-dimensional structure factors by setting one of the wave numbers to be zero. The structure factor in the direction parallel and perpendicular to the nematic axis ($S(q_\parallel)$ and $S(q_\perp)$) are given respectively by:

$$S(q_\parallel) = \frac{2}{Q^2(q_\parallel)}[e^{Q(q_\parallel)} - 1 + Q(q_\parallel)] \tag{16a}$$

with $Q(q_\parallel) = \langle R_g^2 \rangle q_\parallel^2[1 + 2(s_p + (m\text{-}1)s_{p*})/m]$ and

$$S(q_\perp) = \frac{2}{Q^2(q_\perp)}[e^{Q(q_\perp)} - 1 + Q(q_\perp)] \tag{16b}$$

with $Q(q_\perp) = \langle R_g^2 \rangle q_\perp^2[1 + (s_p + (m-1)s_{p*})/m]$

Work by Kempe et al.[13] shows that the SANS data of the end-on SCLCPs can be well fitted by eq in both the parallel and the perpendicular directions. Other groups[45,46] have made similar findings, although they point out that eq is a good approximation only on the large length scale (i.e., low q region when $\langle R_g^2 \rangle q^2 < 1$).

4. Conclusions

In this paper, we have presented a unified model for describing the chain conformation and the phase transition of both side-on and end-on SCLCPs. The interaction between the polymer chain backbone and the LC side groups is treated in our model through two coupling effects: the global nematic coupling and the local hinge effect. The global coupling involves the interaction of a backbone segment with the average nematic field produced by all

LC side groups in its vicinity whereas the hinge effect involves the instantaneous values of the orientation vectors of the chain segment and its own attached LC side group, which is purely an intrachain effect.

The global and local couplings, reflecting the structure of the SCLCPs (e.g., spacer length, backbone flexibility, and etc.), play a key role in determining the chain conformation and phase behavior of the SCLCPs systems. The nematic field controls the chain conformation through both these two coupling effects. The coupling effects on the chain anisotropy are different between the side-on and end-on SCLCPs. For the side-on SCLCPs, these two coupling effects act cooperatively so that the chain conformation is always prolate. For the end-on SCLCPs, these two effects act competitively. The chain conformation can be either oblate or prolate in this case, and depends on the relative strengths of these two couplings. Because of this competition, the chain conformation anisotropy in the end-on SCLCPs is significantly milder than the side-on SCLCPs. The LC grafting density affects the conformation and phase behavior by controlling the relative importance between the LC attached and the LC-free segments. For the side-on SCLCPs, the chain conformation becomes less prolate as the grafting density decreases. For the end-on SCLCPs with low grafting density, the chain conformation can change from oblate to prolate as the grafting density increases. On the other hand, the chain conformation also affects the nematic field primarily through the global coupling. The prolate conformation for the case of end-on SCLCPs enhances the nematic field and therefore increases the phase transition temperature, whereas the oblate conformation frustrates the field and leads to a decrease in the transition temperature. We find that once the temperature is scaled by the transition temperature (which depends on all the coupling coefficients), the nematic order parameter is primarily a function of the reduced temperature, and is not explicitly sensitive to the coupling effects.

In this work, we have only considered the self-coupling within the attached pairs of the chain segment and the LC side group. In this model, the adjacent segments, even in the nematic phase, are uncorrelated in their orientation; i.e., there are no penalty for hairpin turns. Backbone rigidity is limited to one Kuhn segment. The current model can therefore only be applied to SCLCPs systems where the chain conformation does not strongly deviate from a random coil. From scattering experiments, it appears that all the end-on SCLCPs, and side-on SCLCPs with low grafting density, satisfy this requirement.[7] However, for the side-on SCLCPs with very high grafting density (the "jacketed molecule"), the chain can become stiff below some transition temperature.[8] Such a coil−rod transition would require higher-order coupling terms in the intrachain coupling. For example, one can construct coupling between the adjacent LC-attached and LC-free chain segments of the following type:

$$g_C(\{\mathbf{p}_i, \mathbf{q}_i\}) = -\sum_{i=1}^{N} u_C(\mathbf{p}_{(i-1)m+1}\cdot\mathbf{q}_{(i-1)m+1})^2 - \sum_{i=1}^{N} w_C(\mathbf{p}_{(i-1)m+1}\cdot\mathbf{q}_{(i-1)m+1})^2[(\mathbf{p}_{(i-1)m}\cdot\mathbf{p}_{(i-1)m+1}) + (\mathbf{p}_{(i-1)m+1}\cdot\mathbf{p}_{(i-1)m+2})] \quad (17)$$

For $w_C > 0$, such a coupling function would provide energetic penalty when the chain segment is aligned opposite to their adjacent LC-attached segment, i.e. $\mathbf{p}_{(i\text{-}1)m}\cdot\mathbf{p}_{(i\text{-}1)m+1} < 0$. The effect is more significant for side-on SCLCPs than end-on SCLCPs (which is captured by the prefactor $(\mathbf{p}_{(i\text{-}1)m+1}\cdot\mathbf{q}_{(i\text{-}1)m+1})^2$. in the second term of eq 17). With this modification, one can expect that the chain conformation will be elongated in the nematic phase due to energetic penalty for hairpins. As different chain lengths provide different distances for the coupling effects to propagate along, dependence of the transition temperature and the conformational anisotropy on the chain length, observed in experiments, may also be predicted.[47]

Our current model can also be easily applied to multicomponent systems, such SCLCP solutions, blends and block copolymers.[5,6] The added component provides another degree of freedom to adjust the relative strength of the global and the local coupling effects. Moreover, there will in general be phase separation or microphase separation in these multicomponent systems. For the SCLCP blends or solutions, it is straightforward to apply the current bulk-phase model to determine phase equilibrium. Extension to spatially varying systems, such as microphase separation in block copolymers can also be contemplated using the more general set of self-consistent field equations derived in our work, with proper accounting for the block connectivity. These generalizations will be left for future efforts.

Acknowledgment. This work is supported by the National Science Foundation through MRSEC-CALTECH.

References and Notes

(1) Donald, A. M.; Windle, A. H.; Hanna, S. *Liquid Crystalline Polymers*, 2nd ed; Cambridge University Press: Cambridge, U.K., 2005.
(2) Ciferri, A., Krigbaum, W. R., Meyer, R. B., Ed. *Polymer Liquid Crystal*; Academic: New York, 1982.
(3) de Gennes, P. G.; Prost, J. *The Physics of Liquid Crystals*, 2nd ed; Clarendon Press: Oxford, U.K., 1993.
(4) McArdle, C. B., Ed. *Side Chain Liquid Crystal Polymers*; Blackie: Glasgow, 1989.
(5) Kempe, M. D.; Scruggs, N. R.; Verduzco, R.; Lal, J.; Kornfield, J. A. *Nat. Mater.* **2004**, *3*, 177–182.
(6) Kempe, M. D.; Verduzco, R.; Scruggs, N. R.; Kornfield, J. A. *Soft Mater.* **2006**, *2*, 422–431.
(7) Cotton, J. P.; Hardouin, F. *Prog. Polym. Sci.* **1997**, *22*, 795–828.
(8) Lecommandoux, S.; Achard, M. F.; Hardouin, F.; Brulet, A.; Cotton, J. P. *Liq. Cryst.* **1997**, *22*, 549–555.
(9) Leroux, N.; Keller, P.; Achard, M. F.; Noirez, L.; Hardouin, F. *Phys. II Fr.* **1993**, *3*, 1289–1296.
(10) Noirez, L.; Keller, P.; Davidson, P.; Hardouin, F.; Cotton, J. P. *J. Phys.* (*Fr.*) **1988**, *49*, 1993–1999.
(11) Davidson, P.; Noirez, L.; Cotton, J. P.; Keller, P. *Liq. Cryst.* **1991**, *10*, 111–118.
(12) Mattoussi, H.; Ober, R. *Macromolecules* **1990**, *23*, 1809–1816.
(13) Kempe, M. D.; Kornfield, J.; Lal, J. *Macromolecules* **2004**, *37*, 8730–8738.
(14) Rousseau, D.; Marty, J. D.; Mauzac, M.; Martinoty, P.; Brandt, A.; Guenet, J. M. *Polymer* **2003**, *44*, 2049–2055.
(15) Finkelmann, H.; Ringsdorf, H.; Siol, W.; Wendorff, J. H. *ACS Symp. Ser.* **1978**, *74*, 12.
(16) Finkelmann, H.; Rehage, G. *Adv. Polym. Sci.* **1984**, *60−61*, 97–172.
(17) Craig, A. A.; Imrie, C. T. *Macromolecules* **1995**, *28*, 3617–3624.
(18) Craig, A. A.; Imrie, C. T. *Macromolecules* **1999**, *32*, 6215–6220.
(19) Onsager, L. *Ann. N.Y. Acad. Sci.* **1949**, *51*, 627–659.
(20) Flory, P. J. *Proc. R. Soc. London* **1956**, *A234*, 73–89.
(21) Warner, M.; Gunn, J. M. F.; Baumgartner, A. B. *J. Phys. A* **1985**, *18*, 3007–3026.
(22) Wang, X. J.; Warner, M. *J. Phys. A* **1986**, *19*, 2215–2227.
(23) Wang, X. J.; Warner, M. *J. Phys. A* **1987**, *20*, 713–731.
(24) Renz, W.; Warner, M. *Proc. R. Soc. London* **1988**, *A417*, 213–233.
(25) Wang, X. J. *Prog. Polym. Sci.* **1997**, *22*, 735–764.
(26) Odijk, T. *Macromolecules* **1986**, *19*, 2313–2329.
(27) Vroege, G. J.; Odijk, T. *Macromolecules* **1988**, *21*, 2848–2858.
(28) Liu, A. J.; Fredrickson, G. H. *Macromolecules* **1993**, *26*, 2817–2824.
(29) Lee, S.; Oertli, A. G.; Gannon, M. A.; Liu, A. J.; Pearson, D. S.; Schmidt, H. W.; Fredrickson, G. H. *Macromolecules* **1994**, *27*, 3955–3962.
(30) Spakowitz, A. J.; Wang, Z.-G. *J. Chem. Phys.* **2003**, *119*, 13113–13128.
(31) Pryamitsyn, V.; Ganesan, V. *J. Chem. Phys.* **2004**, *120*, 5824–5838.

(32) Olsen, B. D.; Shah, M.; Ganesan, V.; Segalman, R. A. *Macromolecules* **2008**, *41*, 6809–6817.
(33) Olsen, B. D.; Jang, S. Y.; Luning, J. M.; Segalman, R. A. *Macromolecules* **2006**, *39*, 4469–4479.
(34) Brochard, F.; Jouffroy, J.; Levinson, P. *J. Phys.* (*Paris*) **1984**, *45*, 1125–1136.
(35) Chiu, H. W.; Kyu, T. *J. Chem. Phys.* **1995**, *103*, 7471–7481.
(36) Kim, N.; Choi, J.; Chien, L. C.; Kyu, T. *Macromolecules* **2007**, *40*, 9582–9589.
(37) Carri, G. A.; Muthukumar, M. *J. Chem. Phys.* **1998**, *109*, 11117–11128.
(38) Maier, W.; Saupe, A. *Naturforsch.* **1959**, *14a*, 882–889.
(39) Fredrickson, G. H.; Ganesan, V.; Drolet, F. *Macromolecules* **2002**, *35*, 16–39.
(40) Fredrickson, G. H. *The Equilibrium Theory of Inhomogeneous Polymers*; Oxford University Press: Oxford, U.K., 2006.
(41) Rubinstein, M.; Colby, R. H. *Polymer Physics*; Oxford University Press: Oxford, U.K., 2003.
(42) Dubault, A.; Ober, R.; Veyssie, M.; Cabane, B. *J. Phys.* (*Paris*) **1985**, *46*, 1227–1232.
(43) The independence of the transition temperature on the local coupling strength in the absence of the global coupling can be demonstrated mathematically. We omit the proof here, however.
(44) Higgins, J. S.; Benoit, H. *Polymers and Neutron Scattering*; Clarendon Press: Oxford, U.K., 1994.
(45) Zhao, Y. Q.; Jamieson, A. M.; Olson, B. G.; Yao, N.; Dong, S. S.; Nazarenko, S.; Hu, X. S.; Lal, J. *J. Polym. Sci., Part B: Polym. Phys.* **2006**, *44*, 2412–2424.
(46) Brulet, A.; Fourmaux-Demange, V.; Cotton, J. P. *Macromolecules* **2001**, *34*, 3077–3080.
(47) Fourmaux-Demange, V.; Boue, F.; Brulet, A.; Keller, P.; Cotton, J. P. *Macromolecules* **1998**, *31*, 801–806.